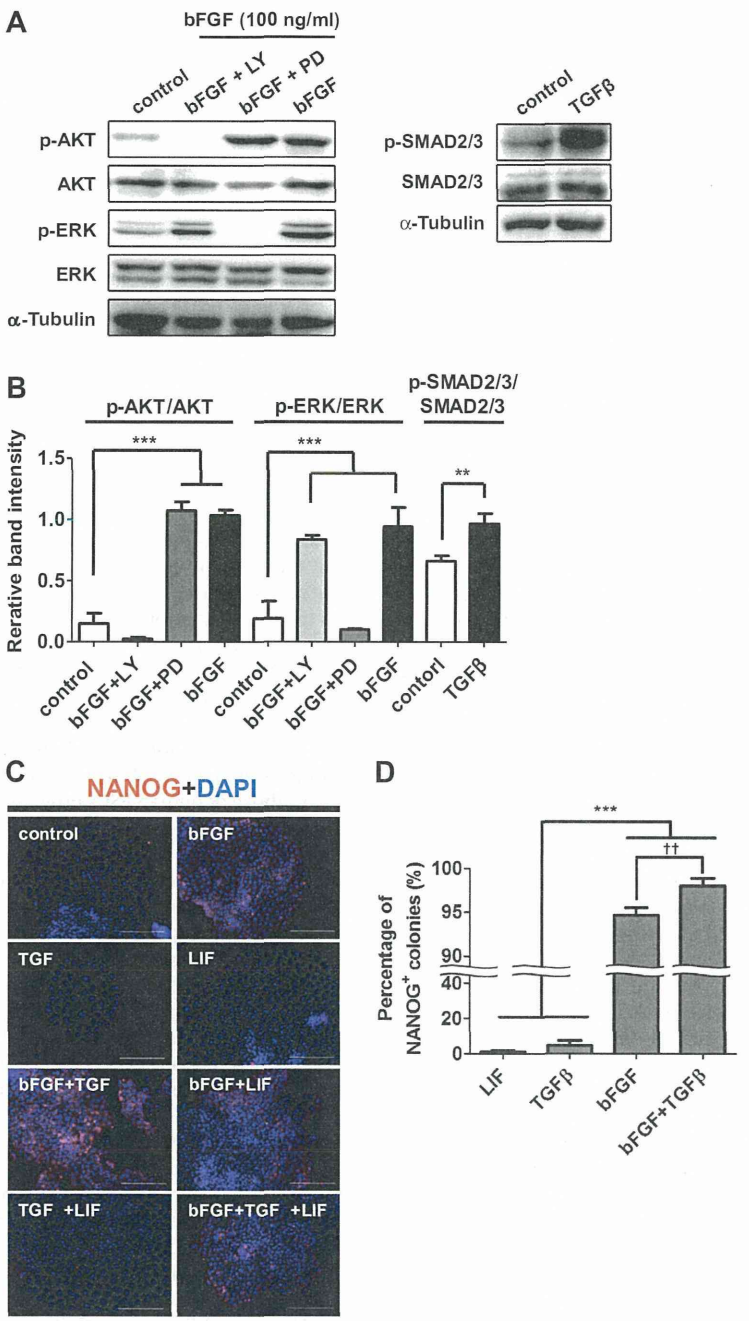


**Fig. 3.** bFGF and TGFβ maintain the undifferentiated state of CM ESCs under feeder-free conditions. (A) Western blot showing the activation of AKT, ERK1/2 and SMAD2/3 by 100 ng/ml of bFGF or 2 ng/ml of TGFβ for 30 min in CM ESCs. CM40 were starved of growth factors overnight and then pre-treated with LY294002 or PD0325901for 1 h before stimulation with bFGF. AKT, ERK1/2, SMAD2/3, and α-Tubulin are shown as loading controls. The relative band intensities of p-AKT/AKT, p-ERK/ERK and p-SMAD2/3/SMAD2/3 are shown in (B). Band intensities were measured by ImageJ software. Data are shown as the mean±SD. One-way ANOVA followed by the Tukey's post-hoc test was used to test inter-group differences. $^{**}P < 0.01$ and $^{***}P < 0.005$. (C) Immunocytochemical analyses of NANOG expression in CM ESCs (CM40) cultured with various growth factors for 4 days. Merged images of NANOG (red) and nuclei (DAPI; blue) are shown. Scale bars represent 200 μm. NANOG expression in cells cultured without any growth factors is shown as a control. (D) Proportion of $NANOG^+$ colonies. The percentage of $NANOG^+$ colonies cultured with various growth factors was analyzed by immunocytochemistry. For statistical analyses, 300 colonies were examined in each experiment ($n = 3$). Data are shown as the mean ± SD. One-way ANOVA followed by the Tukey's post-hoc test was used to test inter-group differences. $^{***}P < 0.005$. The difference between bFGF- and bFGF+TGFβ-treated cells was statistically analyzed using the Student's *t*-test. $^{††}P < 0.01$.

significantly more colonies, suggesting that dissociation-induced apoptosis of CM ESCs occurred and was suppressed by Y27632 (Supplementary Figs. S6B and S6C). Thus, we concluded that CM ESCs are similar to human ESCs and mouse EpiSCs.

## 4. Discussion

Recent advances in the field of basic research for pluripotent stem cells such as the generation of ESCs, iPSCs and stimulus-trig-

**Table 1**
The characters of mouse EpiSCs and mouse, human and CM ESCs.

| Morphology of colony | | Mouse ESCs<br>Small, dome | Mouse EpiSCs<br>Large, flat | Human ESCs<br>Large, flat | CM ESCs<br>Large, flat |
|---|---|---|---|---|---|
| Growth factor dependency | LIF | + | – | – | – |
| | bFGF | – | + | + | + |
| | TGFβ/activin | – | + | + | + |
| Marker expression | NANOG | + | + | + | + |
| | OCT3/4 | + | + | + | + |
| | T (brachyury) | – | + | + | + |
| | CER1 | – | + | + | + |
| | EOMES | – | + | + | + |
| | FOXA2 | – | + | + | + |
| | GATA6 | – | + | + | + |
| | SOX17 | – | + | + | + |
| Tolerance to single cell dissociation | | + | – | – | – |
| Contribution in chimera | | + | – | N/D | N/D |

N/D = not determined.

gered acquisition of pluripotency (STAP) cells have given us realistic expectations for human regenerative medicine [22,34–38]. And the need for the development of methods to test new therapeutic approach using such cells is increasing. CM is a useful experimental animal that can suit such needs, and therefore, the characterization of CM ESCs is important. In this study, we investigated essential signaling pathways for the self-renewal of CM ESCs under feeder-dependent and feeder-free culture conditions.

LIF has been widely used to establish and maintain non-human primate ESCs [15,17,18,39–42], although some researchers claim that LIF cannot maintain the self-renewal capacity of these cells [16,41–43]. We found that LIF did not affect the capacity for self-renewal of CM ESCs (Figs. 1 and 3), although it activated the JAK-STAT3 pathway (Supplementary Fig. S3). More extensive studies are needed to further explore the roles of the LIF-JAK-STAT3 pathway in CM ESCs. In our previous report, the expression of LIFR was not found in undifferentiated CM ESCs [15], but it was found in this study after repetitive experiments (Fig. 1A). This discrepancy was considered to be caused by the detection threshold of RT-PCR under different conditions, particularly PCR primers used in our previous report were human LIFR sequence-originated because there were no available marmoset genomic sequence data.

We also found that the self-renewal of CM ESCs cultured on feeder cells was remarkably promoted by bFGF, which is similar to the characteristic of human ESCs (Fig. 1). However, even in the absence of bFGF, most CM ESCs could be maintained in an undifferentiated state by culture on feeder cells, although they showed slower growth compared to those cultured in bFGF containing medium (Fig. 1B and C). This observation indicates that growth factors secreted from feeder cells such as activin, noggin and bFGF, maintain the undifferentiated state of CM ESCs [44,45]. Indeed, CM ESC colonies cultured on low-density feeder cells differentiated within four passages (Supplementary Fig. S1).

Previous studies have demonstrated the critical roles of PI3K-AKT and MEK-ERK pathways in the self-renewal of human ESCs [2–6]. Our results showed that AKT, but not ERK1/2, was activated by the addition of bFGF (5 ng/ml), while ERK1/2 was continuously activated even in the absence of bFGF on feeder support (Fig. 2A). Moreover, inhibition of either MEK-ERK or PI3K-AKT pathways resulted in reduced self-renewal of CM ESCs (Fig. 2 and Supplementary Fig. S7). Therefore, activation of the PI3K-AKT pathway downstream of bFGF as well as the MEK-ERK pathway by unknown mechanisms is required for self-renewal of CM ESCs on feeder support. On the other hand, both AKT and ERK1/2 were activated by the addition of bFGF (100 ng/ml) under feeder-free condition (Fig. 3A and B). And treatment with LY294002 resulted in the elevated expression of endoderm and mesoderm markers, and treatment with PD0325901 caused the reduced expression of these markers, indicating that modulation of these pathways affects the differentiation process in CM ESCs (Supplementary Fig. S8). We are now extensively investigating the effect of these inhibitors on the differentiation process of CM ESCs induced by the treatment with specific cytokines and EB formation assay.

Several studies have demonstrated differences in the mechanisms of ESC self-renewal between mice and humans. Mouse ESCs require LIF for their self-renewal, whereas human ESCs require bFGF and TGFβ. Mouse EpiSCs originating from post-implantation embryos depend on bFGF and TGFβ, and show characteristics similar to those of human ESCs originating from the inner cells mass of blastocysts as shown in Table 1 [7,8,10]. Mouse EpiSCs are therefore considered to be the counterpart of human ESCs. In this study, we demonstrated that CM ESCs were very similar to human ESCs and mouse EpiSCs in terms of their morphology, gene expression, growth factor dependency for self-renewal, and vulnerability to single cell dissociation.

Our findings strongly suggest that CM ESCs are phenotypically similar to human ESCs. Therefore, CM ESCs may facilitate the development of valuable preclinical experimental systems to test new therapeutic modalities for incurable human diseases, particularly in the field of regenerative medicine.

## Acknowledgments

We thank Michiko Ushijima for administrative assistance, Yoko Nagai and the members of Tani laboratory for their constructive criticisms and technical support. This work was supported by a grant from the Project for Realization of Regenerative Medicine (K. Tani, 08008010) and KAKENHI (T. Marumoto, 23590465) from the Ministry of Education, Culture, Sports, Science and Technology (MEXT), Japan.

## Appendix A. Supplementary data

Supplementary data associated with this article can be found, in the online version, at http://dx.doi.org/10.1016/j.fob.2014.02.007.

## References

[1] Hibino, H. et al. (1999) The common marmoset as a target preclinical primate model for cytokine and gene therapy studies. Blood 93, 2839–2848.
[2] Singh, A.M. et al. (2012) Signaling network crosstalk in human pluripotent cells: a Smad2/3-regulated switch that controls the balance between self-renewal and differentiation. Cell Stem Cell 10, 312–326.
[3] Armstrong, L. et al. (2006) The role of PI3K/AKT, MAPK/ERK and NFκβ signalling in the maintenance of human embryonic stem cell pluripotency and

viability highlighted by transcriptional profiling and functional analysis. Hum. Mol. Genet. 15, 1894–1913.
[4] Li, J. et al. (2007) MEK/ERK signaling contributes to the maintenance of human embryonic stem cell self-renewal. Differentiation 75, 299–307.
[5] Na, J., Furue, M.K. and Andrews, P.W. (2010) Inhibition of ERK1/2 prevents neural and mesendodermal differentiation and promotes human embryonic stem cell self-renewal. Stem Cell Res. 5, 157–169.
[6] McLean, A.B. et al. (2007) Activin a efficiently specifies definitive endoderm from human embryonic stem cells only when phosphatidylinositol 3-kinase signaling is suppressed. Stem Cells 25, 29–38.
[7] Tesar, P.J., Chenoweth, J.G., Brook, F.A., Davies, T.J., Evans, E.P., Mack, D.L., Gardner, R.L. and McKay, R.D.G. (2007) New cell lines from mouse epiblast share defining features with human embryonic stem cells. Nature 448, 196–199.
[8] Brons, I.G.M. et al. (2007) Derivation of pluripotent epiblast stem cells from mammalian embryos. Nature 448, 191–195.
[9] James, D., Levine, A.J., Besser, D. and Hemmati-Brivanlou, A. (2005) TGFβ/activin/nodal signaling is necessary for the maintenance of pluripotency in human embryonic stem cells. Development 132, 1273–1282.
[10] Greber, B. et al. (2010) Conserved and divergent roles of FGF signaling in mouse epiblast stem cells and human embryonic stem cells. Cell Stem Cell 6, 215–226.
[11] Vallier, L., Alexander, M. and Pedersen, R.A. (2005) Activin/Nodal and FGF pathways cooperate to maintain pluripotency of human embryonic stem cells. J. Cell Sci. 118, 4495–4509.
[12] Williams, R.L. et al. (1988) Myeloid leukaemia inhibitory factor maintains the developmental potential of embryonic stem cells. Nature 336, 684–687.
[13] Niwa, H., Burdon, T., Chambers, I. and Smith, A. (1998) Self-renewal of pluripotent embryonic stem cells is mediated via activation of STAT3. Genes Dev. 12, 2048–2060.
[14] Takahashi, K., Murakami, M. and Yamanaka, S. (2005) Role of the phosphoinositide 3-kinase pathway in mouse embryonic stem (ES) cells. Biochem. Soc. Trans. 33, 1522.
[15] Sasaki, E. et al. (2005) Establishment of novel embryonic stem cell lines derived from the common marmoset (Callithrix jacchus). Stem Cells 23, 1304–1313.
[16] Thomson, J.A., Kalishman, J., Golos, T.G., Durning, M., Harris, C.P. and Hearn, J.P. (1996) Pluripotent cell lines derived from common marmoset (Callithrix jacchus) blastocysts. Biol. Reprod. 55, 254–259.
[17] Müller, T., Fleischmann, G., Eildermann, K., Mätz-Rensing, K., Horn, P.A., Sasaki, E. and Behr, R. (2009) A novel embryonic stem cell line derived from the common marmoset monkey (Callithrix jacchus) exhibiting germ cell-like characteristics. Hum. Reprod. 24, 1359–1372.
[18] Shimada, H. et al. (2012) Efficient derivation of multipotent neural stem/progenitor cells from non-human primate embryonic stem cells. PLoS One 7, e49469.
[19] Maeda, T., Kurita, R., Yokoo, T., Tani, K. and Makino, N. (2011) Telomerase inhibition promotes an initial step of cell differentiation of primate embryonic stem cell. Biochem. Biophys. Res. Commun. 407, 491–494.
[20] Shimoji, K. et al. (2010) G-CSF promotes the proliferation of developing cardiomyocytes in vivo and in derivation from ESCs and iPSCs. Cell Stem Cell 6, 227–237.
[21] Chen, H. et al. (2008) Common marmoset embryonic stem cell can differentiate into cardiomyocytes. Biochem. Biophys. Res. Commun. 369, 801–806.
[22] Takahashi, K., Tanabe, K., Ohnuki, M., Narita, M., Ichisaka, T., Tomoda, K. and Yamanaka, S. (2007) Induction of pluripotent stem cells from adult human fibroblasts by defined factors. Cell 131, 861–872.
[23] Niwa, H., Ogawa, K., Shimosato, D. and Adachi, K. (2009) A parallel circuit of LIF signalling pathways maintains pluripotency of mouse ES cells. Nature 460, 118–122.
[24] Levenstein, M.E., Ludwig, T.E., Xu, R.H., Llanas, R.A., VanDenHeuvel-Kramer, K., Manning, D. and Thomson, J.A. (2006) Basic fibroblast growth factor support of human embryonic stem cell self-renewal. Stem Cells 24, 568–574.
[25] Xu, R.H., Peck, R.M., Li, D.S., Feng, X., Ludwig, T. and Thomson, J.A. (2005) Basic FGF and suppression of BMP signaling sustain undifferentiated proliferation of human ES cells. Nat. Methods 2, 185–190.
[26] Xu, C. et al. (2005) Basic fibroblast growth factor supports undifferentiated human embryonic stem cell growth without conditioned medium. Stem Cells 23, 315–323.
[27] Dahéron, L., Opitz, S.L., Zaehres, H., Lensch, W.M., Andrews, P.W., Itskovitz-Eldor, J. and Daley, G.Q. (2004) LIF/STAT3 signaling fails to maintain self-renewal of human embryonic stem cells. Stem Cells 22, 770–778.
[28] Wu, Y., Zhang, Y., Mishra, A., Tardif, S.D. and Hornsby, P.J. (2010) Generation of induced pluripotent stem cells from newborn marmoset skin fibroblasts. Stem Cell Res. 4, 180–188.
[29] Warthemann, R., Eildermann, K., Debowski, K. and Behr, R. (2012) False-positive antibody signals for the pluripotency factor OCT4A (POU5F1) in testis-derived cells may lead to erroneous data and misinterpretations. Mol. Hum. Reprod. 18, 605–612.
[30] Chen, G. et al. (2011) Chemically defined conditions for human iPSC derivation and culture. Nat. Methods 8, 424–429.
[31] Amit, M., Carpenter, M.K., Inokuma, M.S., Chiu, C.-P., Harris, C.P., Waknitz, M.A., Itskovitz-Eldor, J. and Thomson, J.A. (2000) Clonally derived human embryonic stem cell lines maintain pluripotency and proliferative potential for prolonged periods of culture. Dev. Biol. 227, 271–278.
[32] Ohgushi, M. et al. (2010) Molecular pathway and cell state responsible for dissociation-induced apoptosis in human pluripotent stem cells. Cell Stem Cell 7, 225–239.
[33] Watanabe, K. et al. (2007) A ROCK inhibitor permits survival of dissociated human embryonic stem cells. Nat. Biotechnol. 25, 681–686.
[34] Takahashi, K. and Yamanaka, S. (2006) Induction of pluripotent stem cells from mouse embryonic and adult fibroblast cultures by defined factors. Cell 126, 663–676.
[35] Thomson, J.A., Itskovitz-Eldor, J., Shapiro, S.S., Waknitz, M.A., Swiergiel, J.J., Marshall, V.S. and Jones, J.M. (1998) Embryonic stem cell lines derived from human blastocysts. Science 282, 1145–1147.
[36] Evans, M.J. and Kaufman, M.H. (1981) Establishment in culture of pluripotential cells from mouse embryos. Nature 292, 154–156.
[37] Obokata, H., Wakayama, T., Sasai, Y., Kojima, K., Vacanti, M.P., Niwa, H., Yamato, M. and Vacanti, C.A. (2014) Stimulus-triggered fate conversion of somatic cells into pluripotency. Nature 505, 641–647.
[38] Obokata, H. et al. (2014) Bidirectional developmental potential in reprogrammed cells with acquired pluripotency. Nature 505, 676–680.
[39] Shimozawa, N., Nakamura, S., Takahashi, I., Hatori, M. and Sankai, T. (2010) Characterization of a novel embryonic stem cell line from an ICSI-derived blastocyst in the African green monkey. Reproduction 139, 565–573.
[40] Simerly, C.R. et al. (2009) Establishment and characterization of baboon embryonic stem cell lines: An Old World Primate model for regeneration and transplantation research. Stem Cell Res. 2, 178–187.
[41] Suemori, H. et al. (2001) Establishment of embryonic stem cell lines from cynomolgus monkey blastocysts produced by IVF or ICSI. Dev. Dyn. 222, 273–279.
[42] Thomson, J.A., Kalishman, J., Golos, T.G., Durning, M., Harris, C.P., Becker, R.A. and Hearn, J.P. (1995) Isolation of a primate embryonic stem cell line. Proc. Nat. Acad. Sci. 92, 7844–7848.
[43] Mitalipov, S., Kuo, H.C., Byrne, J., Clepper, L., Meisner, L., Johnson, J., Zeier, R. and Wolf, D. (2006) Isolation and characterization of novel rhesus monkey embryonic stem cell lines. Stem Cells 24, 2177–2186.
[44] Wang, G. et al. (2005) Noggin and bFGF cooperate to maintain the pluripotency of human embryonic stem cells in the absence of feeder layers. Biochem. Biophys. Res. Commun. 330, 934–942.
[45] Beattie, G.M., Lopez, A.D., Bucay, N., Hinton, A., Firpo, M.T., King, C.C. and Hayek, A. (2005) Activin A maintains pluripotency of human embryonic stem cells in the absence of feeder layers. Stem Cells 23, 489–495.

Published OnlineFirst April 10, 2014; DOI: 10.1158/2326-6066.CIR-13-0143

Cancer Immunology Research

# TLR7 Ligand Augments GM-CSF–Initiated Antitumor Immunity through Activation of Plasmacytoid Dendritic Cells

Megumi Narusawa, Hiroyuki Inoue, Chika Sakamoto, et al.

*Cancer Immunol Res* Published OnlineFirst April 10, 2014.

Published OnlineFirst April 10, 2014; DOI: 10.1158/2326-6066.CIR-13-0143

Research Article

Cancer Immunology Research

# TLR7 Ligand Augments GM-CSF–Initiated Antitumor Immunity through Activation of Plasmacytoid Dendritic Cells

Megumi Narusawa[1], Hiroyuki Inoue[1,2,3], Chika Sakamoto[1], Yumiko Matsumura[1], Atsushi Takahashi[1], Tomoko Inoue[1], Ayumi Watanabe[1], Shohei Miyamoto[1], Yoshie Miura[1], Yasuki Hijikata[3], Yoshihiro Tanaka[3], Makoto Inoue[5], Koichi Takayama[2], Toshihiko Okazaki[4], Mamoru Hasegawa[5], Yoichi Nakanishi[2], and Kenzaburo Tani[1,3]

## Abstract

Vaccination with irradiated granulocyte macrophage colony-stimulating factor (GM-CSF)–transduced autologous tumor cells (GVAX) has been shown to induce therapeutic antitumor immunity. However, its effectiveness is limited. We therefore attempted to improve the antitumor effect by identifying little-known key pathways in GM-CSF–sensitized dendritic cells (GM-DC) in tumor-draining lymph nodes (TDLN). We initially confirmed that syngeneic mice subcutaneously injected with poorly immunogenic Lewis lung carcinoma (LLC) cells transduced with Sendai virus encoding GM-CSF (LLC/SeV/GM) remarkably rejected the tumor growth. Using cDNA microarrays, we found that expression levels of type I interferon (IFN)–related genes, predominantly expressed in plasmacytoid DCs (pDC), were significantly upregulated in TDLN-derived GM-DCs and focused on pDCs. Indeed, mouse experiments demonstrated that the effective induction of GM-CSF–induced antitumor immunity observed in immunocompetent mice treated with LLC/SeV/GM cells was significantly attenuated when pDC-depleted or IFNα receptor knockout ($IFNAR^{-/-}$) mice were used. Importantly, in both LLC and CT26 colon cancer–bearing mice, the combinational use of imiquimod with autologous GVAX therapy overcame the refractoriness to GVAX monotherapy accompanied by tolerability. Mechanistically, mice treated with the combined vaccination displayed increased expression levels of CD86, CD9, and Siglec-H, which correlate with an antitumor phenotype, in pDCs, but decreased the ratio of $CD4^+CD25^+FoxP3^+$ regulatory T cells in TDLNs. Collectively, these findings indicate that the additional use of imiquimod to activate pDCs with type I IFN production, as a positive regulator of T-cell priming, could enhance the immunologic antitumor effects of GVAX therapy, shedding promising light on the understanding and treatment of GM-CSF–based cancer immunotherapy. *Cancer Immunol Res; 2(6); 1–13. ©2014 AACR.*

## Introduction

In recent clinical trials of patients with diverse solid cancers, cancer immunotherapy such as therapeutic vaccination with granulocyte macrophage colony-stimulating factor (GM-CSF) gene-transduced tumor vaccines (GVAX), as well as sipuleucel-T (Provenge; Dendreon), the first FDA-approved GM-CSF–based therapeutic dendritic cell (DC) vaccine for prostate cancer, induced antitumor immune responses with tolerability (1–3). However, the efficacy of this therapy alone is not satisfactory, raising an urgent need to improve the antitumor effect of GVAX. Although GM-CSF signaling is essential in conventional DC (cDC) maturation, which leads to effective generation of tumor-associated antigen (TAA)-specific T cells and differentiation, the underlying molecular mechanism of how GM-CSF sensitizes and matures DCs (GM-DC, i.e., GM-CSF–sensitized DCs) to trigger host antitumor immunity remains unclear.

Therefore, in this study, we attempted to improve the antitumor effects of GVAX therapy through identification of the key cluster genes upregulated in GM-DCs that operate T-cell priming in tumor-draining lymph nodes (TDLN) by conducting a cDNA microarray analysis. We used a syngeneic Lewis lung carcinoma (LLC)–bearing mouse, which exhibited remarkable tumor regression following subcutaneous administration of fusion (F) gene-deleted nontransmissible Sendai virus vector–mediated GM-CSF gene-transduced LLC (LLC/SeV/GM) cells (4). Using this experimental system, the expression microarray analysis elucidated that pathways involving Toll-like receptor 7 (TLR7) and interferon regulatory factor 7 (IRF7), which induce type I interferon (IFN) production in plasmacytoid DCs (pDC; ref. 5), were upregulated in GM-CSF–activated mature DCs. Further activation of this pathway using

**Authors' Affiliations:** [1]Department of Molecular Genetics, Medical Institute of Bioregulation; [2]Research Institute for Diseases of the Chest, Graduate School of Medical Sciences; [3]Department of Advanced Cell and Molecular Therapy and [4]Center for Clinical and Translational Research, Kyushu University Hospital, Kyushu University, Fukuoka; and [5]DNAVEC Corporation, Tsukuba, Japan

**Note:** Supplementary data for this article are available at Cancer Immunology Research Online (http://cancerimmunolres.aacrjournals.org/).

**Corresponding Author:** Kenzaburo Tani, Department of Molecular Genetics, Medical Institute of Bioregulation, Kyushu University, 3-1-1 Maidashi, Higashi-ku, Fukuoka 812-8582, Japan. Phone: 81-92-642-6449; Fax: 81-92-642-6444; E-mail: taniken@bioreg.kyushu-u.ac.jp

**doi:** 10.1158/2326-6066.CIR-13-0143

Published OnlineFirst April 10, 2014; DOI: 10.1158/2326-6066.CIR-13-0143



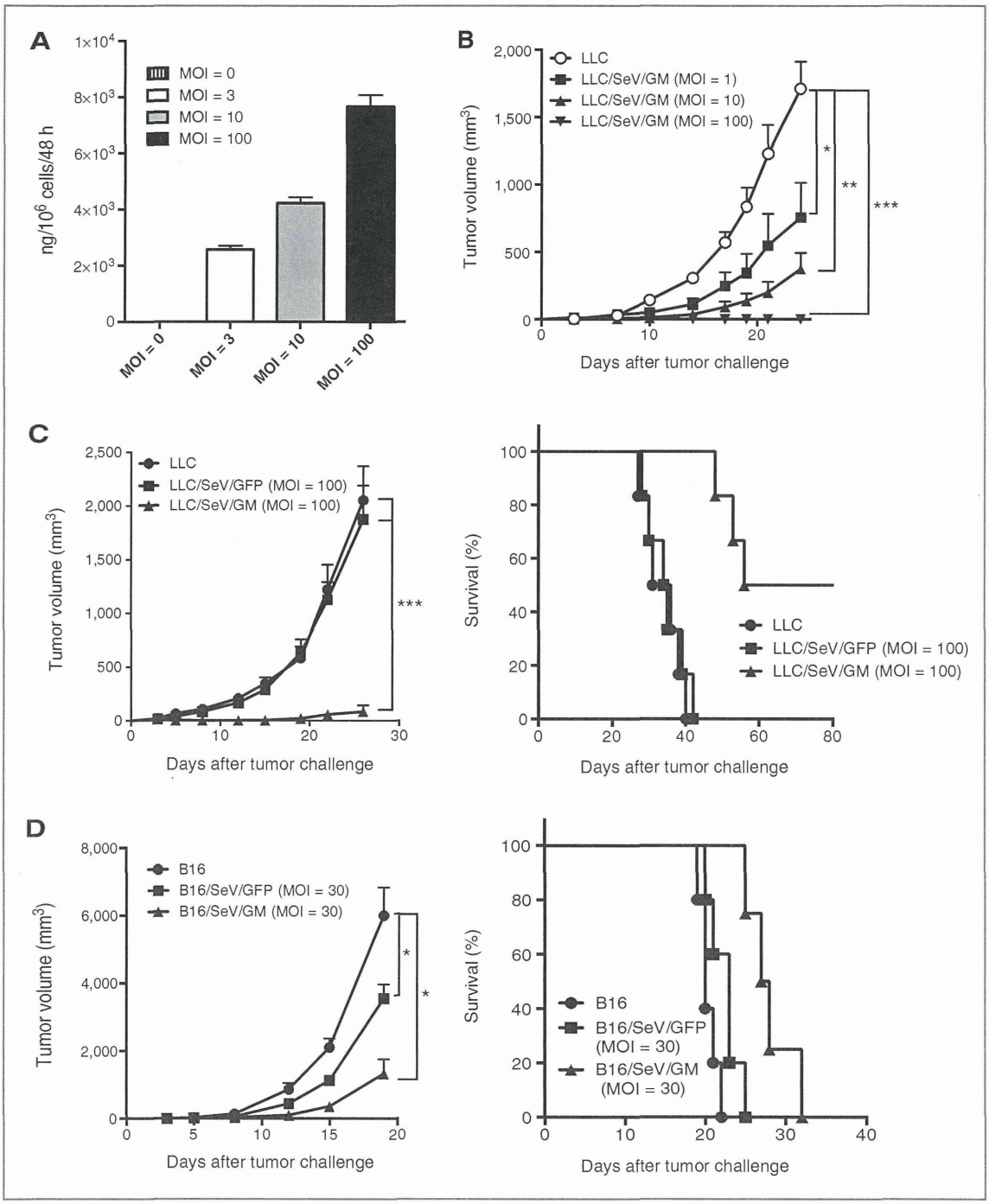


Figure 1. Tumor development of poorly immunogenic LLC and B16F10 cells modified to produce GM-CSF was markedly inhibited. A, dose-escalation studies to assess GM-CSF production from LLC/SeV/GM cells (MOI = 0, 3, 10, and 100). GM-CSF production levels in the supernatants from the 48-hour culture were measured by ELISA. B and C, tumorigenicity assays using LLC cells. B, a total of $3.0 \times 10^5$ LLC and LLC/SeV/GM (MOI of 1, 10, or 100) cells were subcutaneously inoculated into the right flank of C57/BL6N mice ($n = 3$). C, a total of $2.0 \times 10^5$ LLC, LLC/SeV/GFP, or LLC/SeV/GM (MOI = 100) cells were inoculated into the right flank of C57/BL6N mice ($n = 6$). Significant tumor regression (left) and prolonged survival (right) was shown in mice treated with LLC/SeV/GM cells. D, tumorigenicity assays using B16F10 cells. In total, $1.0 \times 10^5$ B16F10, B16/SeV/GFP, or B16/SeV/GM (MOI = 30) cells were inoculated into the right flanks of C57/BL6N mice ($n = 6$). Significant tumor regression (left) and prolonged survival (right) were observed in mice treated with B16/SeV/GM cells. The asterisks indicate statistically significant differences (*, $P < 0.05$; **, $P < 0.01$; ***, $P < 0.001$). Kaplan–Meier survival curves are shown, and mortality was determined by the log-rank test (LLC vs. LLC/SeV/GM and LLC/SeV/GFP vs. LLC/SeV/GM; $P < 0.001$, LLC vs. LLC/SeV/GFP; $P = 0.67$, B16 vs. B16/SeV/GM and B16/SeV/GFP vs. B16/SeV/GM; $P < 0.05$).

Published OnlineFirst April 10, 2014; DOI: 10.1158/2326-6066.CIR-13-0143



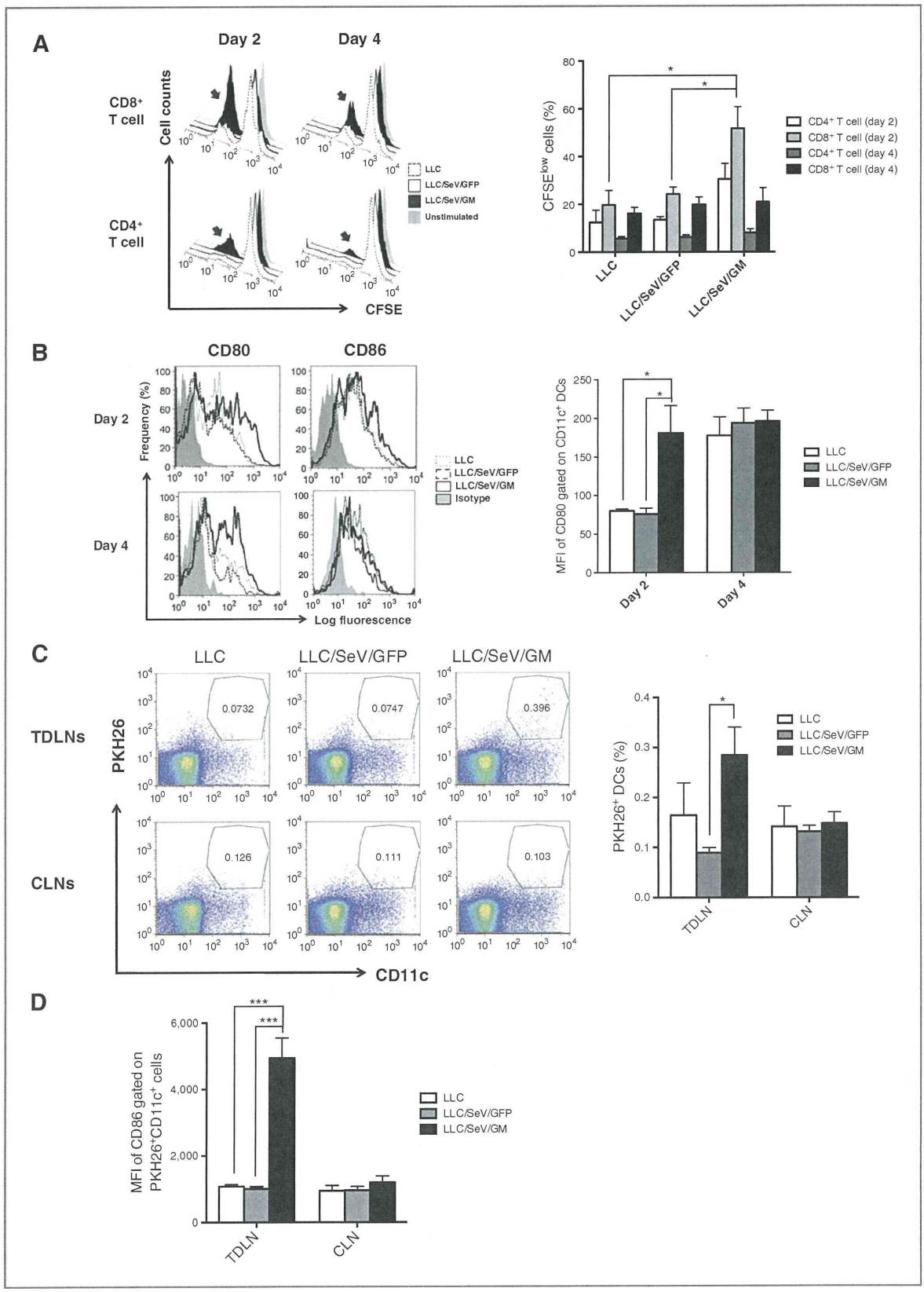

Published OnlineFirst April 10, 2014; DOI: 10.1158/2326-6066.CIR-13-0143



**Table 1.** Canonical pathways identified by IPA

| Pathways | −log (*P* value) | Molecules |
|---|---|---|
| Role of pattern recognition receptors in recognition of bacteria and viruses | 7.42E+00 | OAS1, C3, OAS2, IL6, CCL5, Oas1f, OAS3, IFNA1/IFNA13, TLR2, IFIH1, IRF7, DDX58, TLR7, PIK3R6, EIF2AK2 |
| Pathogenesis of multiple sclerosis | 5.33E+00 | CXCL10, CXCL9, CCL4, CCL5, CXCL11 |
| Activation of IRF by cytosolic pattern recognition receptors | 4.38E+00 | DHX58, IFIH1, IRF7, DDX58, ZBP1, STAT2, IL6, IFIT2, IFNA1/IFNA13, ISG15 |
| IFN signaling | 3.96E+00 | IFIT3, IFIT1, OAS1, MX1, IFI35, STAT2, IFNA1/IFNA13 |
| DC maturation | 3.01E+00 | FCGR2A, HLA-DMB, IL6, MAPK13, FCGR2B, TREM2, IFNA1/IFNA13, FCGR1A, TLR2, COL1A2, IL1RN, FSCN1, PIK3R6, STAT2 |
| Hepatic fibrosis/hepatic stellate cell activation | 2.58E+00 | COL1A2, CXCL3, FN1, CXCL9, IGF1, PDGFA, CCL21, CD14, MMP13, CCL5, IL6, IFNA1/IFNA13 |
| Role of hypercytokinemia/hyperchemokinemia in the pathogenesis of influenza | 2.49E+00 | CXCL10, CCL4, IL1RN, CCL5, IL6, IFNA1/IFNA13 |
| Communication between innate and adaptive immune cells | 2.47E+00 | CXCL10, TLR2, CCL4, IL1RN, TLR7, CCL5, IL6, IFNA1/IFNA13, Ccl9 |
| Role of tissue factor in cancer | 2.45E+00 | F10, PDIA2, PIK3R6, HCK, MMP13, F7, LIMK2, MAPK13, FGR, F2 |
| LXR/RXR activation | 2.26E+00 | APOE, SCD, C3, MSR1 (includes EG:20288), IL1RN, LPL, CLU, CD14, IL6, GC |

TLR7 agonist enhanced the therapeutic antitumor effects of GVAX therapy using irradiated autologous GM-CSF gene-transduced vaccine cells in both LLC and CT26 tumor-bearing mouse models with augmented pDC activation. These results showed that the combination of GVAX and imiquimod is an effective therapeutic strategy for cancer immunotherapy, and indicate that activated pDCs have a critical role in the GM-CSF–induced induction of antitumor immunity.

## Materials and Methods

### Mice

Five- to 10-week-old female immunocompetent C57/BL6N and BALB/cN mice were purchased from Charles River Laboratories Japan and housed in the animal maintenance facility at Kyushu University (Fukuoka, Japan). Type I IFN receptor knockout ($IFNAR^{-/-}$) mice were purchased from The Jackson Laboratory. All animal experiments were approved by the Committee of the Ethics on Animal Experiments in the Faculty of Medicine, Kyushu University. Mouse experiments were carried out at least twice to confirm results.

### Tumor cell lines

LLC and CT26 cells were purchased from the American Type Culture Collection (ATCC) and passaged for 3 to 4 months after resuscitation. The mouse melanoma cell line (B16F10) was a kind gift from Dr. Shinji Okano (Kyushu University) and was validated as free from *Mycoplasma* infection; no other validations were performed. Both LLC and CT26 cells were validated as free from *Mycoplasma* infection. No other validations were performed; besides, the former were found as free from ectromelia virus. LLC and B16F10 cells were maintained in Dulbecco's Modified Eagle Medium (DMEM; Nakalai Tesque) supplemented with 10% heat-inactivated fetal bovine serum (FBS) and 1% antibiotic mixture (Nakalai Tesque). CT26 was maintained in RPMI-1640 (Nakalai Tesque) supplemented with 10% FBS and 1% antibiotic mixture.

### Gene transduction with nontransmissible recombinant Sendai virus vectors

LLC, B16F10, or CT26 cells were infected with nontransmissible Sendai virus vectors encoding green fluorescence protein (GFP) or mouse GM-CSF (SeV/GFP or SeV/GM, respectively), which were prepared by DNAVEC Corp. (6), at the indicated multiplicity of infection (MOI) for 90 minutes (termed as LLC/SeV/GFP, LLC/SeV/GM, B16/SeV/GFP, B16/SeV/GM, or CT26/SeV/GM cells, respectively). They were cultured for 48 hours after viral gene transduction and used for following mouse studies.

Figure 2. GM-CSF–sensitized DCs elicited superior capacities to stimulate T-cell proliferation and to mobilize TAA-phagocytosed mature DCs into TDLNs. A, CFSE-labeled allogeneic MLR assay. Irradiated $CD11c^{+}$ DCs from mice treated with indicated tumor challenge were mixed with CFSE-labeled allogeneic T cells. After 3 days of coculture, the proliferation rates of T cells were assessed by flow cytometric analysis. Representative histograms depict CFSE expression of allogeneic $CD4^{+}CD3^{+}$ or $CD8^{+}CD3^{+}$ T cells (left). Bar graphs, mean + SEM percentage of CFSE-diluted cells/total indicated T cells (right). B, representative histograms depict frequency distributions of MFI of CD80 or CD86 expression in $CD11c^{+}$ DCs from indicated mouse groups on day 2 or 4 after the tumor challenge (left). Bar graphs, mean + SEM of MFI of CD80 on DCs in TDLNs (right). C, representative dot plots show $PKH26^{+}CD11c^{+}$ cells gated by their FSC/SSC profiles in TDLNs or CLNs (left). Bar graphs, mean + SEM of percentage of $CD11c^{+}PKH26^{+}$ cells in TDLNs or CLNs (right). D, bar graphs, mean + SEM of MFI of CD86 expression levels in $PKH26^{+}CD11c^{+}$ cells (*, $P < 0.05$; ***, $P < 0.001$).

Published OnlineFirst April 10, 2014; DOI: 10.1158/2326-6066.CIR-13-0143



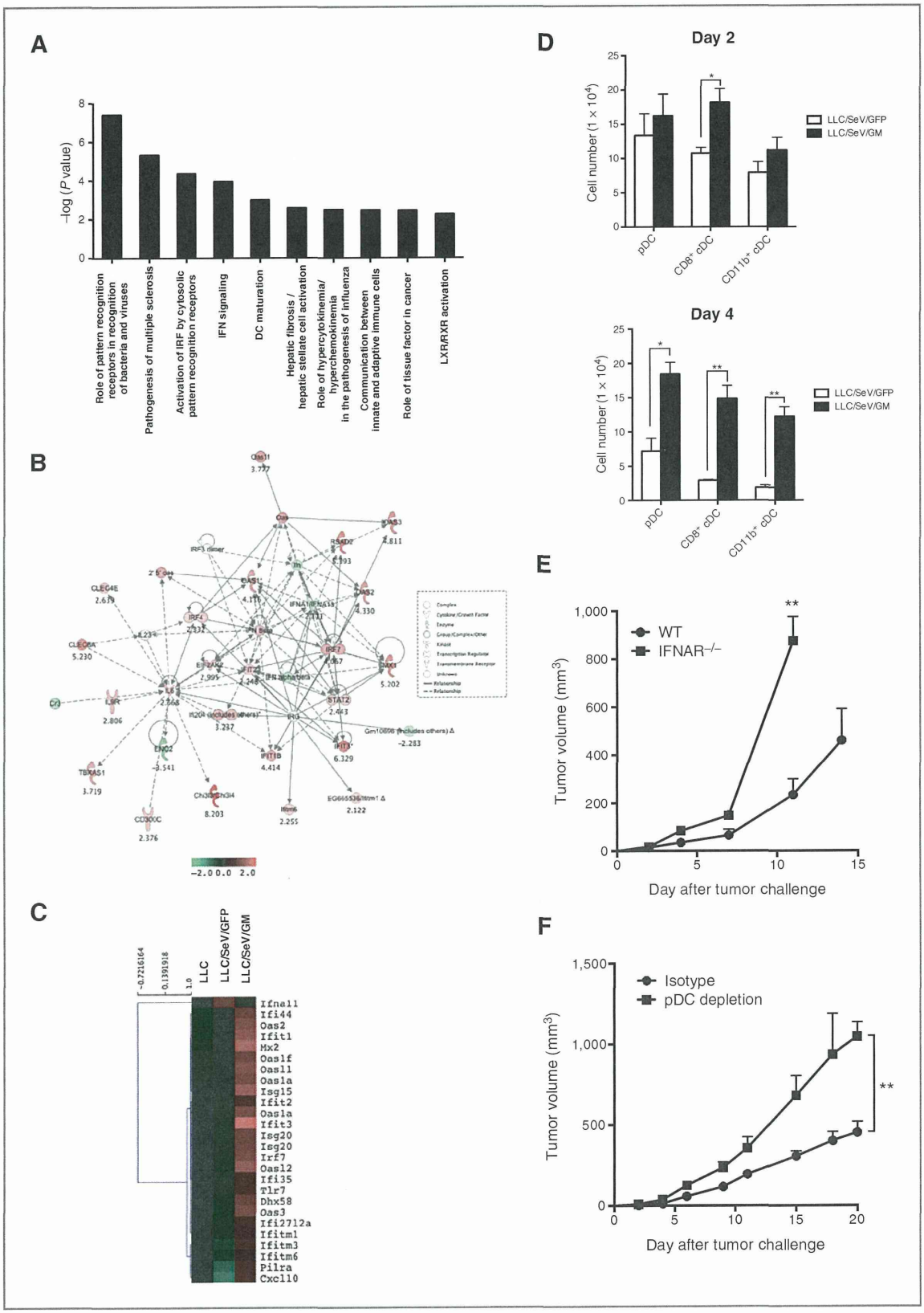

Published OnlineFirst April 10, 2014; DOI: 10.1158/2326-6066.CIR-13-0143



### *In vivo* experiments

For tumorigenicity assays, syngeneic C57/BL6N mice were subcutaneously challenged with $2.0 \times 10^5$ LLC, LLC/SeV/GFP, or LLC/SeV/GM cells with or without imiquimod (R-837; 50 μg/mouse; Invivogen) or lipopolysaccharide (LPS; 5 μg/mouse; Sigma-Aldrich) resuspended in 100-μL Hanks' Balanced Salt Solution (HBSS; Life Technologies) in the right or left flank. To dissect the role of type I IFN and pDCs in the tumorigenicity assays, $IFNAR^{-/-}$ or pDC-depleted mice were subcutaneously challenged with $2.0 \times 10^5$ LLC/SeV/GM cells in the right flank. For therapeutic tumor vaccination assays, LLC/SeV/GFP, LLC/SeV/GM, and CT26/SeV/GM cells were irradiated at 50 Gy and were designated as irLLC/SeV/GFP, irLLC/SeV/GM, and irCT26/SeV/GM cells, respectively. On days 2 and 9 after tumor challenge with parental LLC or CT26 cells, C57/BL6N or BALB/cN mice were subcutaneously vaccinated with the indicated tumor vaccine cells in the opposite flank. Tumor volume was measured every 2 to 4 days and calculated with the following formula: 0.4 × (largest diameter) × (smallest diameter)$^2$.

### ELISA assay

*In vitro* expression levels of mouse GM-CSF produced from LLC, LLC/SeV/GFP, or LLC/SeV/GM cells at the MOI and time points were measured using mouse GM-CSF enzyme-linked immunosorbent assay (ELISA) kits (R&D Systems).

### Flow cytometric analysis

TDLNs, spleen, and tumor vaccine sites (TVS) harvested from the indicated groups of mice ($n = 3$–5) were homogenized and filtered through a 100-μm cell strainer (BD Biosciences). For splenocyte preparation, smashed spleens were treated with ammonium chloride to lyse red blood. For T-cell detection in mixed lymphocyte reaction (MLR) assays, cells were stained with anti-CD4 (RM4.5)–PE (eBioscience), anti-CD3e–APC (145-2C11), and anti-CD8a–PerCP (53-6.7; BioLegend). For phenotypic analyses of DCs in TDLNs, cells were stained with an anti-mouse CD11c Ab [anti-CD11c–APC (N418); BioLegend] in combination with anti-mouse Abs, including anti-B220–PE (RA3-6B2), anti-CD317 (PDCA-1, BST2)–PE (eBio129c; all eBioscience), anti-CD80–PE (16-10A1), anti-CD8a–PerCP, anti-CD86–FITC (GL-1), or anti-CD11b–FITC (M1/70; all BioLegend). For phenotypic analyses of pDCs in TDLNs, cells were stained with either anti-CD317 (PDCA-1, BST2)–PE, anti-PDCA-1–APC (JF05-1C2.4.1; Miltenyi Biotec), or anti-CD11c–PerCPCy5.5 (N418; eBioscience) in combination with anti-mouse Abs, including anti-CD86–FITC, anti-CD9–FITC (MZ3; BioLegend), and anti-Siglec-H–FITC (551.3D3; Miltenyi Biotec). For regulatory T-cell (Treg) detection in TDLNs, cells were permeabilized with Cytofix/Cytoperm kit (BD Biosciences), washed with BD Perm/Wash buffer (BD Biosciences), and stained with anti-CD4, anti-CD25–FITC (PC61.5), and anti-FoxP3–APC (FJK-16s; all eBioscience). Cells were incubated with Abs and analyzed with BD FACSCalibur flow cytometer, CellQuest software (BD Biosciences), and FlowJo software (TreeStar).

### Allogeneic MLR assays

To prepare $CD11c^+$ DCs as stimulators, on day 2 of the tumorigenicity assay, $CD11c^+$ DCs were purified from TDLNs in mice treated with LLC, LLC/SeV/GFP, or LLC/SeV/GM cells using CD11c MicroBeads (Miltenyi Biotec). To prepare the pDC subset as stimulators, total bone marrow cells harvested from naïve C57/BL6N mice were cultured in RPMI-1640 supplemented with 50 ng/mL murine Fms-related tyrosine kinase 3 ligand (Flt3L; PeproTech) for 8 days and Siglec-H–positive cells (pDCs) were purified using anti-Siglec-H–FITC Ab and anti-FITC MicroBeads (Miltenyi Biotec). Sorted pDCs were then incubated overnight with or without 2.5 μg/mL of imiquimod or 10 ng/mL of murine recombinant GM-CSF (PeproTech). To prepare allogeneic T cells as responders, T cells were sorted from splenocytes harvested from naïve BALB/cN mice using a Pan T-cell isolation kit II (Miltenyi Biotec). A total of $5.0 \times 10^4$ responder T cells labeled with 1.0 μmol/L CFSE [5(6)-carboxyfluorescein diacetate N-succinimidylester; Sigma-Aldrich] were cocultured with an equal number of 30 Gy–irradiated $CD11c^+$ DCs. A total of $2.0 \times 10^5$ T cells labeled with 2.5 μmol/L of CFSE were cocultured with $4.0 \times 10^4$ of pDCs for 5 days. The proliferation rate of the gated $CD3^+$ T-cell fraction was visualized by CFSE dilution.

### Detection of DCs that engulfed TAAs

LLC, LLC/SeV/GFP, and LLC/SeV/GM cells were labeled with the PKH26 Red Fluorescent Cell Linker Mini Kit (Sigma-Aldrich), respectively, according to the manufacturer's instruction. On day 2 after they were subcutaneously injected into the right flanks of mice, axillary lymph nodes in both TDLNs and CLNs were harvested, incubated with anti-CD86–FITC and anti-CD11c–APC Abs, and subjected to flow cytometric analysis.

### cDNA microarray

Dead cells were excluded from $CD86^+CD11c^+$ DCs using 7-AAD viability dye (Beckman Coulter), which were sorted by

Figure 3. Transcriptome analysis suggested the involvement of type I IFN–related pathways in GM-DCs during GM-CSF–induced antitumor immunity. A, total RNA was isolated from $CD86^+$ DCs in TDLNs from mice inoculated with LLC, LLC/SeV/GFP, or LLC/SeV/GM cells 2 days after the tumor challenge and subjected to cDNA microarray. The top 10 canonical pathways significantly upregulated in GM-DCs, in comparison with those in GFP-DCs, by which a right-tailed Fisher exact test was calculated using the entire dataset. B, IPA was performed using the type I IFN pathway–related genes from the original commonly regulated probes differentially expressed between GFP-DCs and GM-DCs. Differentially expressed genes are indicated in red and green, representing up- and downregulation induced by GM-CSF activation, respectively. A high degree of gene regulation is indicated by bold-colored genes. Direct or indirect associations with the differentially expressed genes indicated by no color were not found to be significantly different in this assessment. Positive regulatory interactions are depicted by solid arrows (direct interactions) or dashed arrows (indirect interactions). C, heatmap based on type I IFN pathway–related genes that were differentially expressed in $CD86^+$ DCs in TDLNs from indicated mouse groups. D, cell numbers of DC subsets (pDC, $CD8^+$ cDCs, and $CD11b^+$ cDC) in TDLNs at days 2 (top) and 4 (bottom) after the respective tumor challenge were comparatively quantified (*, $P < 0.05$; **, $P < 0.01$). E and F, representative tumor growth curves observed in $IFNAR^{-/-}$ (E) or pDC-depleted (F) mice (**, $P < 0.01$).